This article has been accepted for publication in IEEE Transactions on Power Electronics. This is the author's version which has not been fully edited and content may change prior to final publication. Citation information: DOI 10.1109/TPEL.2024.3496542

Investigation of Electro-thermo-mechanical Degradation and Crack Propagation of Wire Bonds in Power Modules Using Integrated Phase Field Modelling and Finite Element Analysis

Han Jiang, *Member, IEEE*, Shuibao Liang, *Member, IEEE*, Yaohua Xu, Saranarayanan Ramachandran

***Abstract*—Interfacial fatigue degradation and crack formation of wire bonds are one of the serious issues related to packaging in power modules that affect the reliability of power electronics. This work presents a new approach based on a combination of phase field modelling and finite element analysis to study the electro-thermo-mechanical behavior, the interface degradation and crack propagation processes of wire bonded interconnects in IGBT power modules. The strain energy density obtained from the macro-scale electro-thermo-mechanical analysis is transferred to the mesoscale phase field modelling to study the interface fatigue and crack propagation, considering the effect of wire grain morphology. The temperature and stress distribution characteristics of a typical IGBT power module with Al wire bonds under power cycling are investigated. Stress concentration at the interconnect interface caused by thermal strains between wire and chip is examined. The crack length increases with increasing cycle number. The presence of Al grain boundaries is found to have a significant impact on crack propagation, due to grain boundary energy and weakening effects. The developed model could provide new insights for predicting the lifetime and crack growth of power modules, and offer a pathway for the reliability optimization of wire bonds.**

***Index Terms*—Crack, modelling, power modules, reliability, wire bonds.**

I. Introduction

POWER electronic modules based on insulated-gate bipolar transistor (IGBT) chips are widely used in aerospace, electric vehicles, and energy regeneration systems [1], [2]. With the significant increase in demand and requirements for improved power conversion efficiency [3], more efficient and highly reliable power electronic modules are needed [4], [5]. The trend of miniaturization and high power frequency of power modules has brought many new challenges to the reliability of power module packaging [6], [7]. In serving conditions, IGBT power modules are subject to multi-physics coupling loads [8], Joule heating induced by the current flow can further result in thermal mismatch within the interface interconnect materials [9]. Therefore, the interconnect structures in power modules are subjected to thermal cycling stress, which can contribute to various types of failure modes of modules [10], [11]. Although the alternative Cu and Cu-based wire bonds could offer better performance and longer lifetime than conventional Al wire bonds [12], performance degradation of wire bonds due to deformation [13], thermally induced stress [14], and crack propagation [15], [16] still significantly influences the operating life of power modules. Therefore, revealing the mechanics and characteristics of wire bond failure are particularly important for the lifetime analysis and prediction of power modules.

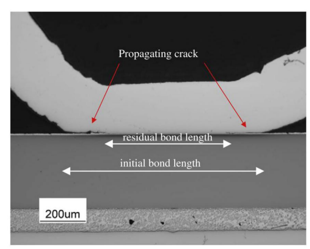

Fig. 1. The typical morphology of crack formation and propagation of wire bonds in a power module [17].

The typical observation of crack propagation near wire bonds in power modules is shown in Fig. 1, in which the effective wire bond length keeps decreasing during thermal cycling [17]. It is known that the thermo-mechanical and crack failure of wire bonds are significantly affected by the loop geometry and layout [18], the bonding angle and loop height are confirmed to be the predominant factors that affect the performance of the bond wires [19], thus the loop geometry could be optimized to decrease the plastic deformation and improve the reliability of wire bonds. Generally, the wire bonds in power modules are directly connected with the metallization layer on the chip. The significant difference in thermal expansion coefficient between different materials can result in that the wire tip and heel (see Fig. 1) suffering from

Manuscript received XXXX; revised XXXX; accepted XXXX. Date of publication XXXX; date of current version XXXX. The work was supported in part by the Foundation for Introduction of High-Level Talents of Anhui University (S020318029/019) and the University Synergy Innovation Program of Anhui Province (GXXT-2022-080); in part by the Research Foundation for the Introduction of Talent of Hefei University of Technology (13020-03712023005), Anhui Provincial Natural Science Foundation (2308085QE165) and the Natural Science Foundation of China (62404068, 62404001). The review of this article was arranged by Editor XXX. (Corresponding author: Shuibao Liang.)

Han Jiang and Yaohua Xu are with School of Integrated Circuits, Anhui University, Hefei 230601, China (e-mail: h.jiang@ahu.edu.cn, h.jiang2@lboro.ac.uk; xyh@ahu.edu.cn)

Shuibao Liang is with School of Materials Science and Engineering, Hefei University of Technology, Hefei 230009, China (e-mail: s.liang@hfut.edu.cn)

Saranarayanan Ramachandran is with Advanced Forming Research Centre, University of Strathclyde, Renfrew PA4 9LJ, U.K. (e-mail: saranarayanan.ramachandran@strath.ac.uk)

This article has been accepted for publication in IEEE Transactions on Power Electronics. This is the author's version which has not been fully edited and content may change prior to final publication. Citation information: DOI 10.1109/TPEL.2024.3496542

high thermal stress [20], which may lead to performance deterioration at the bonding interface for power modules [21]. The experimental endeavours encounter challenges in effectively and dynamically capturing and analyzing the interfacial stress and thermal strain of the wire bonds; consequently, several investigations have been conducted to evaluate the stress characteristics and their influencing factors of wire bonds in power modules based on finite element analysis. For instance, Meng *et al.* [22] used finite element simulation to investigate the stress concentration and residual stress characteristics in the vicinity of the wires within IGBT power modules. Huang *et al.* [23] employed finite element analysis to evaluate the thermomechanical reliability of wire bonds with different wire loops in power modules. Dai *et al.* [24] utilized finite element simulation to study the plastic strain and stress distribution of wire bonds in power modules with different bonding angles, and found that the plastic strain at the bond wire heel was greater with a smaller bonding angle.

For power modules in long-term service, the cyclic thermal stress can induce fatigue damage and eventual failure of the wire bonds in power modules. Thermal fatigue of wire bonds in power modules goes through three stages: micro-crack initiation, macro-crack formation and fracture [25]. The wire bond fatigue issues can be interpreted by interface crack formation and propagation [26]. Additionally, the evaluated plastic strain and stress near the wire bond of power modules can be used to predict the fatigue lifetime based on Coffin–Manson model [27] and the stress-based model [28]. In general, the increase in crack length during propagation can be predicted using finite element analysis methods, which typically rely on Paris' law [29]. The extended finite element method has been effectively applied to predict wire bond crack propagation in power modules [30]. However, the crack propagation rate prediction is mainly based on a predefined crack, and the crack path may not be accurately predicted.

Notably, the microstructure and grain characteristics of the wire bonds depend on the bonding process parameters, subsequently influencing hardness and strength [31]. Moreover, the change in grain distribution and microstructure has significant impacts on the propagation path of cracks in the wire bonds of power modules. The grain size and misorientation between different grains may influence the rate of crack propagation. It has been found that the damage accumulation due to grain boundaries in the wire bonds can cause softening and performance degradation of the bonds [32]. Furthermore, coarsened grains and voids existed in the Al wires may also precipitate bonding failure [33]. In other words, the microstructural morphology of the wire bonds, including grain distribution and defects, is vital to the bonding performance and quality, which greatly affects the reliability of power modules.

However, studies on the impact of grain boundaries on crack propagation in Al wires used in power modules remain limited. Shqair *et al.* [34] developed a cohesive zone model to elucidate the relationship between microstructural alteration and crack path, showing that cracks in wire bonds initiated at the edges and propagated along grain boundaries near the metallization layer. Luo *et al.* [35] employed a cohesive zone model to analyze the microstructural characteristics associated with the performance degradation of the Al wire bonds within power modules. These studies offered effective methods for investigating the impact of grain characteristics on crack growth and performance degradation in wire bonds. Nevertheless, the cohesive zone models typically require predefined crack paths, posing a challenge in accurately capturing the crack initiation process. Therefore, further studies and new approaches are needed to reveal the mechanisms and mechanics of crack formation and propagation influenced by the microstructure of wire bonds in power modules.

The phase field method exhibits promising capabilities for simulating crack formation and propagation in power modules [36]. It eliminates the need for explicitly tracking crack surfaces and possesses the advantage of capturing crack initiation without requiring predefined crack paths [37], [38], thereby showcasing advantages over the method based on cohesive zone models. Some studies investigated the crack propagation in die attach materials within power modules [36], [39], but the model employed ignored the influences of grain boundaries and phase microstructure on performance degradation and crack propagation. Hence, contributions are expected to focus on revealing the impact of grain boundary energy and morphology on the mechanics of interface degradation in wire bonds within power modules. This will be achieved through the development of a modelling method that integrates meso-scale phase field modelling with macro-scale finite element analysis, as explored in this study.

In this work we propose a methodology integrating phase field modelling with electro-thermo-mechanical coupling finite element analysis to examine the impact of grain boundaries in wire bonds on the crack formation and propagation in wire bonds of power modules. The thermo-mechanical behaviour of a typical IGBT power module during the power cycling is studied. Then, the high-stress region adjacent to the Al line is constructed as a sub-model to transfer strain energy density obtained from finite element analysis to the developed phase field model for dynamic capture and investigation of crack initiation and propagation characteristics within the wire bond and interface. Furthermore, the polycrystalline models for the Al wire are established based on the Voronoi tessellation to further investigate the influence of grain boundaries on crack initiation and propagation. Special emphasis will be placed on uncovering the impact of grain boundaries on crack evolution, propagation velocity, and the consequent changes in the mechanical response of Al wire bonds within power modules, aiming to deepen understanding of failure mechanics and optimize performance and reliability in wire bondings. Section II details the coupling relations among all physical fields to be considered and the numerical methodology. Section III investigates temperature and stress variations within power modules during power cycling, then focuses on analyzing crack propagation in Al wire bonds and evaluating the impact of wire grain morphology. Finally, Section IV presents the conclusions drawn from the findings.

II. Methodology

To analyze the electro-thermo-mechanical behavior of power modules and the degradation process of wire bonds

This article has been accepted for publication in IEEE Transactions on Power Electronics. This is the author's version which has not been fully edited and content may change prior to final publication. Citation information: DOI 10.1109/TPEL.2024.3496542

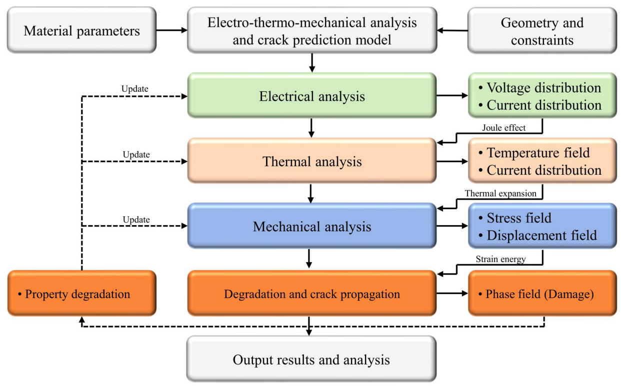

Fig. 2. Flowchart of crack propagation and failure prediction of wire bonds in power modules during power cycling.

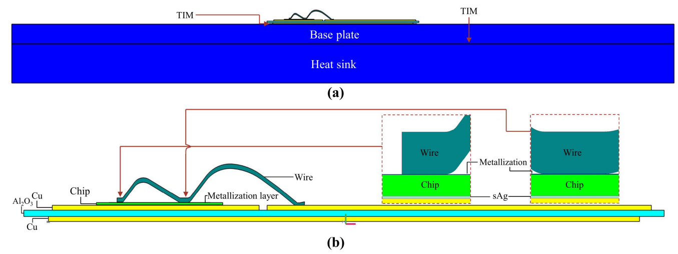

Fig. 3. (a) Schematic diagram of the multi-layer material stack-up of a typical considered power module. (b) Illustration of the portion of the power module for mechanical analysis.

during the power cycling, the employed integrated approach involves several steps: 1) assigning material parameters, establishing models and defining constraints, 2) conducting electro-thermo-mechanical analysis while considering coupling effects, 3) extracting strain energy density, then predicting crack propagation and interface degradation, 4) evaluating performance degradation and accordingly updating material parameters, 5) exporting and analyzing results. Steps two to four are iteratively updated to account for the influence of crack propagation on material properties and the electro-thermo-mechanical behavior. This iterative process is illustrated in a detailed flowchart, as shown in Fig. 2. The four types of fields, i.e., current density, temperature, stress and damage phase fields, are included, and there are coupling effects between the physical fields, ultimately determining the electro-thermo-mechanical behavior and interface degradation of wire bonds in the power modules.

A. Electro-Thermal and Thermo-Mechanical Models

A typical IGBT power module is considered to enable the electro-thermo-mechanical analysis of power modules, as shown in Fig. 3(a). Referring to previous experimental investigations [34], [40], the accelerated condition of 12 power cycles in a DC mode is assumed to be applied at the left surface of the top side copper layer, the right surface of the top side copper layer is grounded. A single cycle consists of a 3-second duration for the power-on stage followed by a 6-second duration for the power-off stage, and the applied current density is set be 1.9×10^7 A/m^2 [41]. The distributions of current density and electric potential in the power module are governed by $\nabla \cdot \overrightarrow{j} = 0$, and $\nabla \cdot [\lambda \cdot \nabla \phi] = 0$, where j is the current density, λ is the electric conductivity, and ϕ is the electric potential.

Joule heating induced by the current density can cause an increase in the temperature of the power module, and the temperature distribution yields

$$\nabla \cdot (k \nabla T) + \lambda |\nabla \phi|^2 + \dot{q} = \rho c_p \frac{\partial T}{\partial t}, \tag{1}$$

where T is the temperature, k is the thermal conductivity, and $\dot{q}$ is the heat source except for Joule heating, ρ is the density, c_p is the specific heat capacity. The bottom surface of the baseplate is cooled with a convection coefficient of 1500 $\mathrm{W/m^2 \cdot K}$ and an ambient temperature of 45 °C [34], an adiabatic condition is applied to the other boundaries [28].

The thermal strain ε_{th} can be calculated by $\varepsilon_{\text{th}} = \int_{T_0}^{T_f} \alpha_{\text{th}} dT$, where α_{th} is the thermal expansion coefficient. Thus, the stress may be written as $\sigma = E \cdot (\varepsilon_{\text{mech}} + \varepsilon_{\text{th}})$, and E is the Young's modulus, $\varepsilon_{\text{mech}}$ is the mechanical strain. The stress distribution in the power module obeys

$$\frac{\partial \sigma_{ij}}{\partial x_j} = 0. \tag{2}$$

Given that the deformation mainly occurs at the layers in the layers of the bottom copper and those above it, this part of the power module is considered to investigate the mechanical behavior, as illustrated in Fig. 3(b). It is assumed that the displacement of the bottom edge of the copper layer along y-aixs is set to 0, and left node of the bottom edge is fixed [34]. The plastic deformation of Cu and Al is characterized by an isotropic hardening model, and the deformation of the die attach sintered silver (sAg) layer is assumed to follow a bilinear kinematic hardening model [24], [42].

B. Degradation and Phase Field Modelling

The phase field fracture model follows the Griffith theory and is used to describe the dynamic degradation process of the wire bonds in the power module. A phase field variable d is introduced to describe the damaged state of the materials, $d = 0$ and $d = 1$ represent intact and damaged domains [43], [44]. Then the main governing equations for stress and phase field variable evolution can be given by

$$\begin{gathered} \nabla \cdot [g(d)\sigma] = 0, \\ \mathcal{G}_c \left(d - \ell^2 \Delta d \right) = (2 - 2d)\ell H, \end{gathered} \tag{3}$$

with boundary condition: $\mathbf{n} \cdot \sigma = \widetilde{\mathbf{t}}$, $\mathbf{u} = \widetilde{\mathbf{u}}$ and $\mathbf{n} \cdot \nabla d = 0$, where $\widetilde{\mathbf{t}}$ and $\widetilde{\mathbf{u}}$ are the traction and displacement on the corresponding boundaries respectively [45], [46]. The degradation function $g(d) = (1-d)^2$, ℓ is the characteristic length, $\mathcal{G}_c$ is the critical energy release rate or fracture toughness, the history field H is the maximum value of tensile strain energy across the present loading time.

To include the fatigue degradation effect, the approach developed by Carrara *et al.* [47] is incorporated into the phase field evolution equation. The fracture toughness $\mathcal{G}_c$ is updated as $\mathcal{G}_\mathrm{d} = f(\bar{\alpha})\mathcal{G}_\mathrm{c}$, and the governing equation for the phase field reads

$$\mathcal{G}_\mathrm{d}\left(d - \ell^2\Delta d\right) - \ell^2\nabla d\cdot\nabla\mathcal{G}_\mathrm{d} = (2-2d)\ell H, \tag{4}$$

where $f(\bar{\alpha})$ is the fatigue degradation function [47], and it can take the following form:

$$f(\bar{\alpha}) = \begin{cases} 1 & \text{if} \quad \bar{\alpha} \le \alpha_T \\ \left(\frac{2\alpha_T}{\bar{\alpha}+\alpha_T}\right)^2 & \text{if} \quad \bar{\alpha} \ge \alpha_T \end{cases}, \tag{5}$$

where $\alpha_T = \mathcal{G}_\mathrm{c}/12\ell$, $\bar{\alpha} = \int_0^t H(\alpha\dot{\alpha})|\dot{\alpha}|d\tau$, $H(\alpha\dot{\alpha})$ is the Heaviside function. $\alpha = g(d)\psi_0^+$, where ψ_0^+ is the active part of the elastic strain energy density.

To verify the effectiveness of the model, an Al specimen with the dimension of H_s=W_s=200 µm, as shown in Fig. 4, is prepared to investigate the crack formation and propagation process. The boundary condition is illustrated in Fig. 4, the bottom edge is fixed, and the predicted crack initiation and crack propagation are presented in Fig. 5. It is observed that the crack forms at a tensile displacement of 0.2 µm, then it propagates in the horizontal direction. The obtained patterns are consistent well with the experimental observation of Al samples [48], [49]. The stress-strain curve of the top boundary is given in Fig. 5(d), it effectively capture the deformation characteristics and crack-induced stress relief stage of the Al.

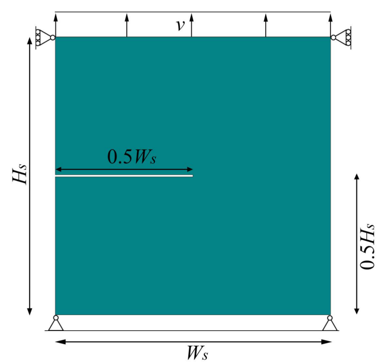

Fig. 4. Boundary condition of an Al sample subjected to tension.

C. Material Parameters

With regard to the materials and layered structure (i.e., Fig. 2) considered in this work, the types of materials and dimensions of each layer are listed in Table I. To investigate the electro-thermal and thermo-mechanical behaviour, the electric, thermal and mechanical properties of the different materials should be assigned, as shown in Table II [24], [34], [50]. The yield stress and tangent modulus of the Al metallization layer are set to be 100 and 502 MPa [50], [51]. In the simulation process for crack investigation, the characteristic length is assigned to be ℓ=1 µm. Although the developed model could potentially be expanded to investigate the crack propagation and failure of various types of wire bonds in power modules, such as Cu and Cu-based wires, the current focus of this investigation will be on Al wire bonds within the considered typical structure. Based on the reported values of the critical

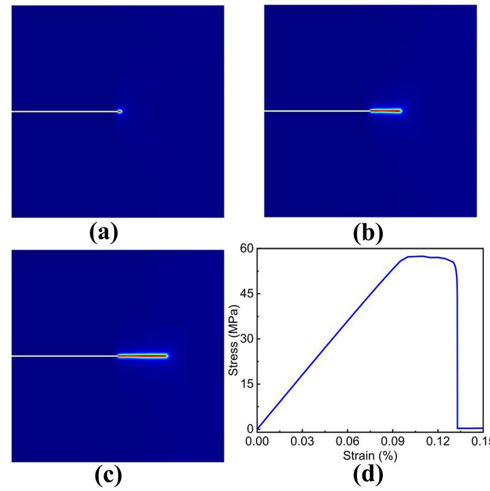

Fig. 5. Simulated crack pattern at a displacement of (a) 0.2, (b) 0.26 and (c) 0.27 µm. (d) Stress-strain response of the sample.

energy release rate for Al [52], [53], $\mathcal{G}_\mathrm{c}$ is estimated to be 65 J/m^2 after considering that the critical energy release rate could depend on the characteristic length ℓ [54].

TABLE I
MATERIALS AND DIMENSIONS OF EACH LAYER

Layer	Material	Length×Width (mm×µm)
Wire	Al	11.2×280
Metallization layer	Al	6.2×5
IGBT chip	Si	7.7×140
Die attach	sAg	7.7×20
Top copper in DBC	Cu	36×300
Ceramic in DBC	Al_2O_3	39×380
Bottom copper in DBC	Cu	36×300
Superior thermal interface	TIM	38×100
Base plate	Al	170×5000
Inferior thermal interface	TIM	170×100
Heat sink	Al	170×10000

TABLE II
MATERIAL PROPERTIES

Parameter	Al	Si	sAg	Cu	Al_2O_3	TIM
Denisty (Kg/m^3)	2700	2330	7350	8960	3780	1180
Electric conductivity (S/m)	3.7e7	55.56	2.5e7	5.9e7	1e-12	1e-20
Thermal conductivity (W/m· K)	238	124	250	390	24	2
Heat capacity (J/Kg· K)	897	750	230	390	830	1044
Thermal expansion coefficient (ppm/K)	23.5	4.1	19.6	17	8	23.5
Poisson's ratio	0.33	0.3	0.37	0.34	0.2	0.33
Young's modulus (GPa)	76	131	6.28	97	370	76
Yield Stress (MPa)	31	–	55	138	–	–
Tangent modulus (MPa)	98.7	–	7000	1350	–	–

This article has been accepted for publication in IEEE Transactions on Power Electronics. This is the author's version which has not been fully edited and content may change prior to final publication. Citation information: DOI 10.1109/TPEL.2024.3496542

D. Numerical Considerations

The simulation is conducted by solving the partial differential equations using the finite element method, implemented with MATLAB and the package COMSOL Multiphysics. The implicit backward difference formula is used for time derivatives, and the equations are solved in a fully coupled approach using the direct PARDISO solver, with Newton's method applied iteratively to handle nonlinearity. Additionally, the solver utilizes adaptive time-stepping, adjusting time step sizes dynamically to meet specified tolerances during computations, with a maximum time step set at 0.05 s. The coupled electro-thermo-mechanical equations can be solved and used to predict the response of materials, and noting the material properties in the potential crack propagation region can be determined using $P_f = g(d)P_s$, where P_s represents the properties of the bulk materials, then the interaction effect between electro-thermo-mechanical finite element analysis and phase field modelling can be incorporated.

III. Results and Discussion

A. Temperature Field and Thermal Stress Distribution

During the power cycling, the predicted junction temperature is plotted in Fig. 6(a). It is observed that the maximum temperature is about 160 °C during the first power cycle, while the maximum temperature reaches 178 °C after several power cycles, closely matching the predictions made by Shqair et al [34]. The elevated temperature is induced by Joule heating when the applied current density is passed through the IGBT chip. Fig. 6(b) presents the temperature distribution of the power module during the power cycling for t=3 s. The temperature is mainly concentrated in the chip domains, and the left part of the power module suffers from high temperatures.

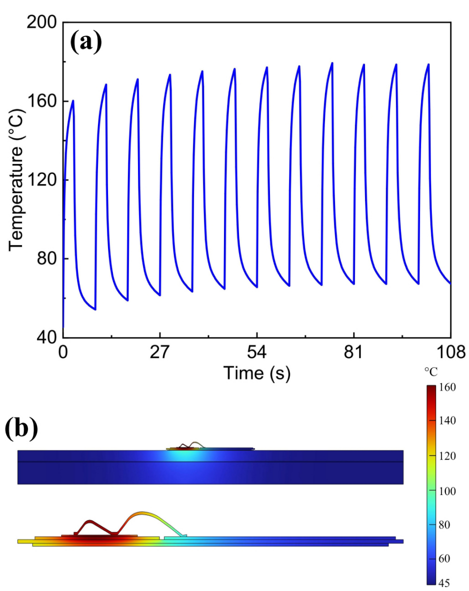

Fig. 6. (a) Predicted junction temperature profile during power cycling. (b) Temperature distribution of the power module after power cycling for 3 s.

The increased temperature of the power modules across the different layers of induces thermal strain mismatch, leading to the thermal stress in the power module, as shown in Fig. 7. Comparing the von Mises stress distribution of the power module after the first cycle to that after 4 cycles, it can be seen that the von Mises stress increases, which is induced by the higher temperature and the accumulated plastic strain. It has been observed that the predicted stress at the metallization layer and direct bond copper is larger than the yield stress of Al and Cu, respectively. Consequently, the plastic deformation of Al metallization and Cu layers can restrict the deformation of other layers, accumulating plastic deformation as the cycle number increases. Fig. 7(b1) and (b2) provide an enlarged view of the stress distribution of the Al wire bond and its interface region. The stress is mainly concentrated at the wire tip and heel adjacent to the Si chip, exhibiting similar characteristics to those observed in other studies [29]. Moreover, the stress near the wire heel is higher than that near the wire tip, which was also demonstrated by a previous study [22].

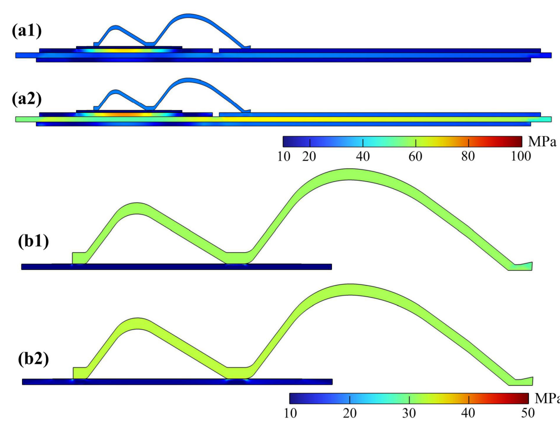

Fig. 7. Von Mises stress distribution of the power module after the power cycling for (a1) 9 and (a2) 36 s. (b1–b2) Stress distribution near the Al wire bonded interconnects at 9 and 36 s, respectively.

B. Crack Propagation of Al Wire Bonds

Noting that the high stress is observed near the interface between Al wire and Si Chip, a subdomain containing the investigated Al/Si interface is selected for examining the processes of crack formation and prorogation, as plotted in Fig. 8, in which the region framed by dotted lines is considered for the degradation prediction.

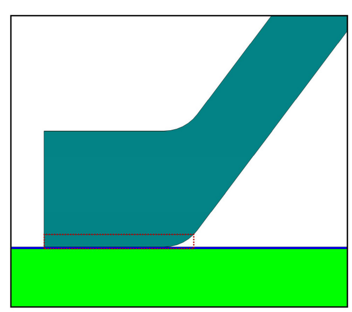

Fig. 8. Schematic diagram of the submodel near the wire bonded interface, with the region enclosed by dotted lines designated for degradation prediction.

This article has been accepted for publication in IEEE Transactions on Power Electronics. This is the author's version which has not been fully edited and content may change prior to final publication. Citation information: DOI 10.1109/TPEL.2024.3496542

Fig. 9 presents simulated crack formation and propagation of the Al wire bond in the power module during power cycling. After the first power cycle, a crack initiates at the heel of the bonding interface, as captured in Fig. 9(a). The simulated results have a good agreement with the experimental observation [55], and the crack propagation near the wire heel is faster than that near the wire tip [34], [56]. As the power cycle number increases, the formed crack grows and expands along the bonding interface. After 8 power cycles, specifically at t=72 s, the residual effective bond length is only half of the initial bond length. After 12 power cycles, the effective length of the wire bonding interface is reduced to one-sixth of its original interconnection length, reducing the mechanical integrity and signal transmission efficiency within the power module, thereby compromising its performance and reliability.

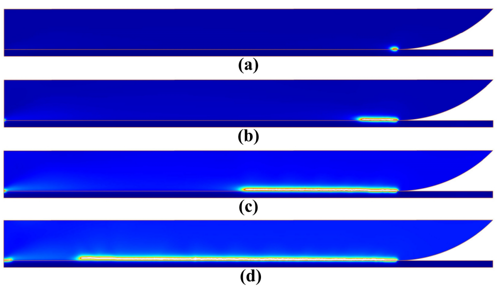

Fig. 9. Simulated crack propagation of the Al wire bonded interconnects in the power module after the power cycling for (a) 9, (b) 36, (c) 72 and (d) 108 s.

The damage induced by the crack formation and propagation along the wire bonding interface induces the degradation of interconnect material properties, thus affecting the mechanical behaviour of the power module. The formed crack can induce the stress relief [57], resulting in the redistribution of stress, as shown in Fig. 10. The location of the maximum stress node changes from right to left along the interface due to the crack propagation. The average stress in the subdomain initially increases and then decreases, with values of 23.24, 35.68, 34.20, and 28.18 MPa at 9, 36, 72, and 108 s, respectively. The formation of the crack induces significant stress relief during the later stages of the crack propagation.

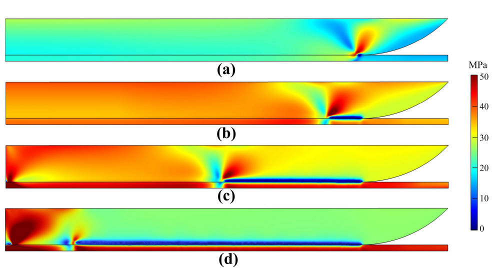

Fig. 10. Von Mises stress distribution of the Al wire bonded interconnects in the power module after the power cycling for (a) 9, (b) 36, (c) 72 and (d) 108 s.

C. Grain Boundary Effect on Electro-thermo-mechanical Degradation

The wires used for bonding in power modules generally have the microstructure of polycrystal grains, and the microstructure characteristics depend on the parameters of the bonding process [58]. The grain boundaries included in the Al wire bonds may provide some favorable paths for crack propagation. Therefore, this subsection considers the polycrystalline structure and grain boundaries within the Al wire. The polycrystalline structure of the Al wire is constructed utilizing the Voronoi tessellation implemented in MATLAB [59], [60], with the grain size varying gradually along the y-axis direction as observed in previous experiments [61]. Given the variation in bonding strength at the wire/metallization-layer interface and the decrease in grain boundary strength over a certain range [34], [62], and considering that the critical energy release rate depends on grain boundary strength and surface energy. We assume that the parameter group for the critical energy release rate at the domains of bulk, wire/metallization-layer interface, and Al grain boundaries is assigned the values (2, 2, 1), (2, 1.5, 1), and (2, 1.5, 0.5) times the initially set $\mathcal{G}_c$ for three cases A, B and C, respectively. These groups are selected to represent different scenarios involving variations in bonding process parameters and fluctuations in grain boundary properties, facilitating the examination of interface crack propagation and performance degradation under varying conditions. Similarly, the crack forms at the wire heel near the bonding interface, as displayed in Fig. 11 (a). The formed crack for Case A tends to propagate along the grain boundaries, as shown in Fig. 11 (b), (c) and (d). For Case B, as depicted in Fig. 12, crack formation and propagation occur slightly faster than in Case A due to the interconnect interface having a lower fracture toughness.

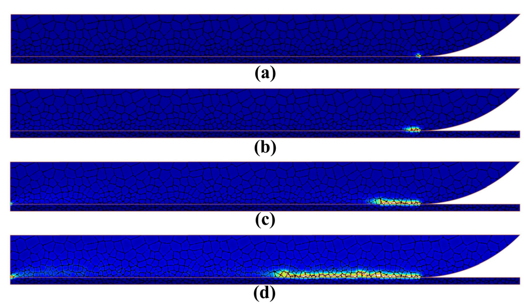

Fig. 11. Simulated crack prorogation of the Al wire bonded interconnects in the power module with considering Case A of grain boundary effect after the power cycling for (a) 9, (b) 36, (c) 72 and (d) 108 s.

Fig. 13 presents the crack prorogation process of the Al wire bonded interconnects in the power module for Case C. It is found that the grain boundary morphology has a significant impact on the pathway of crack evolution due to the decreased critical energy release rate induced by the grain boundaries. From Fig. 13(b), it is seen that the initial crack forms at the interface between the wire heel and the metallization layer, and the formed crack almost always propagates along the grain boundaries. This phenomenon is more pronounced compared to Cases A and B. Furthermore, the reduced fracture

This article has been accepted for publication in IEEE Transactions on Power Electronics. This is the author's version which has not been fully edited and content may change prior to final publication. Citation information: DOI 10.1109/TPEL.2024.3496542

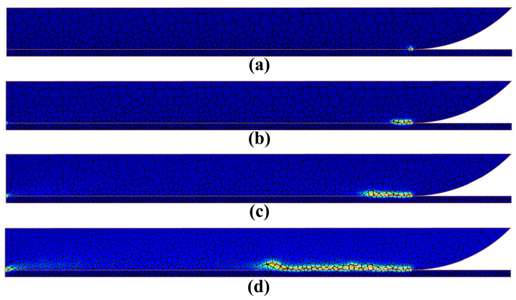

Fig. 12. Simulated crack prorogation of the Al wire bonded interconnects in the power module with considering Case B of grain boundary effect after the power cycling for (a) 9, (b) 36, (c) 72 and (d) 108 s.

toughness at the grain boundaries causes the crack formed on the right to propagate faster to the left. Meanwhile, a new crack emerges near the interface between the wire tip and metallization layer, as depicted in Fig. 13(c). Furthermore, the length of this newly formed crack increases as the number of power cycles reaches 12, as captured in Fig. 13(d). Given that the grain boundaries could be the weakest sites in the Al wire bonds [63], it is reasonable to observe crack propagation occurring alongside the grain boundaries within the wire, as confirmed by experiment [64]. The simulated result of crack formation is prominently displayed in Fig. 13(e), which is in good agreement with the experimental observation shown in Fig. 13(f). Specifically, the high stress between the Al wire and the metallization layer causes crack initiation, but the formed crack propagation subsequently mainly occurs in the Al wire.

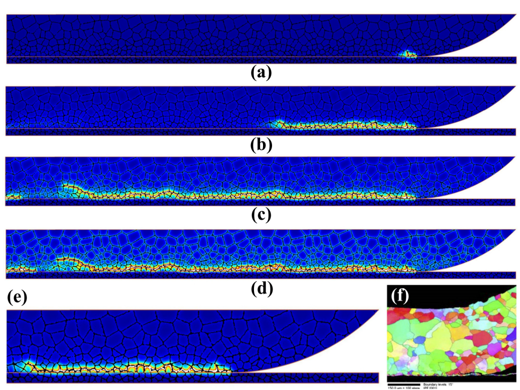

Fig. 13. Simulated crack prorogation of the Al wire bonded interconnects in the power module with considering Case C of grain boundary effect after the power cycling for (a) 9, (b) 36, (c) 72 and (d) 108 s. Comparison of simulated crack (e) and experimentally observed Al wire bond damage (f) [65].

To quantitatively investigate the influence of different parameter group assignments on the crack growth rate, the crack lengths of various cases are calculated, as depicted in Fig. 14. Increasing the duration of power cycling results in a progressive increase in crack length. The high crack growth rate is primarily evident during the power-on stage of each cycle, whereas the crack growth rate decreases as the number of power cycles increases. Moreover, it is noted that the crack length and propagation speed are greatest and fastest in Case C, while Case A exhibits the smallest crack growth rate. In the case where the influence of grain boundaries is not considered, as its fracture toughness is set to half that of the other three cases, the crack length is more prominent than in Cases A and B, but smaller than that of Case C due to the consideration of lower grain boundary fracture toughness in Case C. It should be mentioned that the crack propagation determines the service life and performance of wire bonds, as the effective bond length decreases with crack propagation, leading to a reduced life. Paris' law describes the relationship between crack growth rate per cycle and the stress intensity factor range [26]. The stress intensity factor, which depends on the crack opening displacement and the distance from the crack tip, is usually determined using finite element analysis of the model, including pre-existing cracks in other studies [15]. Despite requiring further detailed analysis of the strain corresponding to different crack states at each moment, the predicted results from the present simulations provide a foundational understanding that could be expanded upon in future work to correlate the service life.

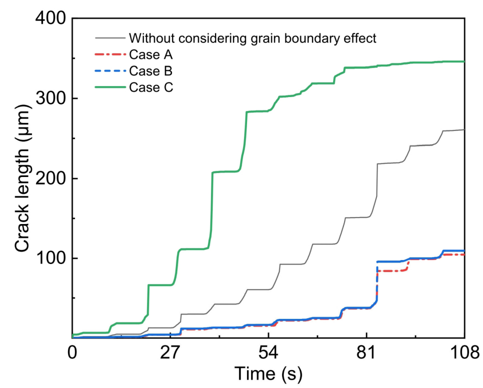

Fig. 14. Increase in the crack length of the Al wire bonded interconnects in the power module during the power cycling.

Furthermore, the von Mises stress of the right edge node (i.e., near the heel) at the Al wire bonded is evaluated, as shown in Fig. 15. It is seen that the magnitude of the stress decreases as the number of power cycles increases, which is mainly induced by the crack propagation and stress relief. The stress of the right edge node in Case A is much higher than those in other cases due to the slower crack propagation rate. The two stages of stress increase and decrease also exhibit periodicity, with the magnitude of stress gradually decreasing over time. After 12 power cycles, the formed cracks result in a significant decrease in the residual bond length, leading to a decrease in the von Mises stress.

IV. CONCLUSION

In this work, a novel approach that integrates phase field modelling and multi-physics finite element analysis is developed to investigate the interface degradation and crack propagation process of Al wire bonds in power modules under power cycling, with incorporating the effect of the electro-thermo-mechanical response. The thermo-mechanical behaviour of the wire bonded interconnect in the power module is firstly investigated, and then the strain energy density obtained from the macro-scale electro-thermo-mechanical

This article has been accepted for publication in IEEE Transactions on Power Electronics. This is the author's version which has not been fully edited and content may change prior to final publication. Citation information: DOI 10.1109/TPEL.2024.3496542

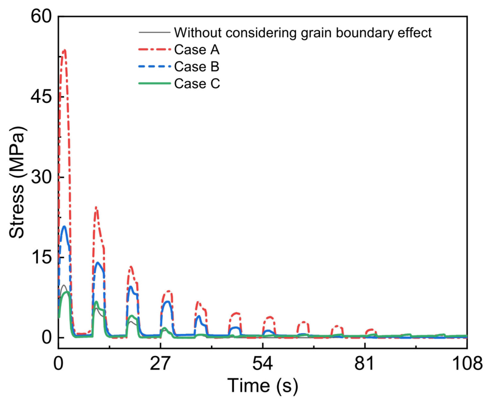

Fig. 15. Evolution of the von Mises stress of the right edge node at the Al wire bonded interface in the power module during the power cycling.

analysis during the power cycling is transferred to the meso-scale phase field modelling to study the crack propagation of the wire bond. Furthermore, with considering the cases where the wire bond possesses non-homogeneous grain distributions, the grain boundary effect on crack propagation and electro-thermo-mechanical degradation is examined. It is found that the elevated temperature induced by Joule heating leads to stress concentration at the wire tip and heel adjacent to the Si chip layer. As the cycle number increases, the accumulation of strain energy density at the stress concentration region is provided as the driving force for crack propagation, resulting in an increase in crack length. The initial crack forms at the interface between the wire heel and the metallization layer; the crack tends to propagate along the Al grain boundaries due to the grain boundary energy and weakening. In the scenario with lower fracture toughness at the grain boundaries, cracks propagate more rapidly, leading to more pronounced stress relief.

The proposed approach incorporates the grain boundary morphology effect through combined phase field modelling and macro finite element analysis to reveal the mechanism and mechanics of interface degradation and crack propagation of Al wire bonds, potentially applicable to other types of wire bonds and offering new insights into the pathway for the reliability optimization of wire bonds in power modules. The present study primarily investigates the crack propagation of wire bonds under high temperature swings, attentions must be given to the specific operating conditions when applying this method to the investigation under low temperature swings due to the potential different deformation mechanisms and degradation of the solder layer. While the simulation results qualitatively agree with previous experiments, further research should concentrate on quantitative verification to clarify the influence of grain morphology on crack propagation and performance degradation of wire bonds in power modules.

References

[1] B. Ji, V. Pickert, W. Cao, and B. Zahawi, "In situ diagnostics and prognostics of wire bonding faults in IGBT modules for electric vehicle drives," *IEEE Trans. Power Electron.*, vol. 28, no. 12, pp. 5568–5577, Mar. 2013.

[2] A. Abuelnaga, M. Narimani, and A. S. Bahman, "A review on IGBT module failure modes and lifetime testing," *IEEE Access*, vol. 9, pp. 9643–9663, Jan. 2021.

[3] L. Wang, W. Wang, K. Zeng, J. Deng, G. Rietveld, and R. J. E. Hueting, "Opportunities and Challenges of Pressure Contact Packaging for Wide Bandgap Power Modules," *IEEE Trans. Power Electron.*, vol. 39, no. 2, pp. 2401–2419, 2024.

[4] Z. Khatir, R. Lallemand, A. Ibrahim, and D. Ingrosso, "Thermal Stress Analysis Comparison in IGBT Power Modules between DC and Switching Power Cycling," *IEEE Trans. Power Electron.*, vol. 38, no. 9, pp. 11 500–11 506, Jun. 2023.

[5] G. Liu, X. Li, Y. Wang, X. Huang, G. Chang, and H. Luo, "A method to derive the coupling thermal resistances at junction-to-case level in multichip power modules," *IEEE Trans. Power Electron.*, vol. 38, no. 2, pp. 1747–1756, Sep. 2023.

[6] W. Lai, M. Chen, L. Ran, S. Xu, N. Jiang, X. Wang, O. Alatise, and P. Mawby, "Experimental Investigation on the Effects of Narrow Junction Temperature Cycles on Die-Attach Solder Layer in an IGBT Module," *IEEE Trans. Power Electron.*, vol. 32, no. 2, pp. 1431–1441, 2017.

[7] C. Chen, A. Suetake, F. Huo, D. Kim, Z. Zhang, M. C. Hsieh, W. Li, N. Wakasugi, K. Takeshita, Y. Yamaguchi, Y. Momose, and K. Suganuma, "Development of SiC Power Module Structure by Micron-Sized Ag-Paste Sinter Joining on Both Die and Heatsink to Low-Thermal-Resistance and Superior Power Cycling Reliability," *IEEE Trans. Power Electron.*, vol. 39, no. 9, pp. 10 638–10 650, 2024.

[8] Y. Huang, Y. Luo, F. Xiao, B. Liu, and X. Tang, "Evaluation of the Degradation in Electrothermal Characteristics of IGBTs During Thermal Cycling Cocaused by Solder Cracking and Al-Wires Lifting-Off Based on Iterative Looping," *IEEE Trans. Power Electron.*, vol. 38, no. 2, pp. 1768–1778, 2023.

[9] X. Ge, K. Chen, H. Wang, Z. Xu, and Z. Fu, "Failure Mechanism Investigations of Bond Wires Lifting-Off and Die-Attach Solder Aging Considering the Thermal Coupling Effects," *IEEE Trans. Power Electron.*, pp. 1–14, 2024.

[10] U. M. Choi, F. Blaabjerg, and S. Jørgensen, "Power cycling test methods for reliability assessment of power device modules in respect to temperature stress," *IEEE Trans. Power Electron.*, vol. 33, no. 3, pp. 2531–2551, May 2018.

[11] L. Xie, E. Deng, S. Yang, Y. Zhang, Y. Zhong, Y. Wang, and Y. Huang, "State-of-the-art of the bond wire failure mechanism and power cycling lifetime in power electronics," *Microelectron. Reliab.*, vol. 147, p. 115060, Aug. 2023.

[12] B. Czerny and G. Khatibi, "Cyclic robustness of heavy wire bonds: Al, AlMg, Cu and CucorAl," *Microelectron. Reliab.*, vol. 88-90, pp. 745–751, 2018.

[13] Z. Zhao, Z. Zhang, S. J. Lawman, Z. Yin, Y. Hu, J. Xu, and Y. Shen, "Characterization of electrical-thermal-mechanical deformation of bonding wires under silicone gel using LF-OCT," *IEEE Trans. Power Electron.*, vol. 36, no. 10, pp. 11 045–11 054, Mar. 2021.

[14] K. B. Pedersen and K. Pedersen, "Dynamic Modeling Method of Electro-Thermo-Mechanical Degradation in IGBT Modules," *IEEE Trans. Power Electron.*, vol. 31, no. 2, pp. 975–986, Apr. 2016.

[15] X. Yang, J. Ye, X. Wu, K. Heng, Y. He, and G. Liu, "Lifetime Prediction for Lift-off of Bond Wires in IGBTs Using Paris Law With Analytical Calculation of Crack Length," *IEEE Trans. Power Electron.*, vol. 38, no. 10, pp. 13 099–13 110, Jul. 2023.

[16] Z. Zhang, C. Chen, A. Suetake, H. Ishino, H. Sampei, T. Endo, K. Sugiura, K. Tsuruta, and K. Suganuma, "Online Condition Monitoring of Solder Fatigue in a Clip-Bonding SiC mosfet Power Assembly via Acoustic Emission Technique," *IEEE Trans. Power Electron.*, vol. 38, no. 2, pp. 1468–1478, Sep. 2023.

[17] P. A. Agyakwa, M. R. Corfield, L. Yang, J. F. Li, V. M. F. Marques, and C. M. Johnson, "Microstructural evolution of ultrasonically bonded high purity Al wire during extended range thermal cycling," *Microelectron. Reliab.*, vol. 51, no. 2, pp. 406–415, Feb. 2011.

[18] Y. Chen, Q. Wu, C. Li, H. Luo, Y. Xia, Q. Yin, W. Li, and X. He, "Thermal Mitigation and Optimization Via Multitier Bond Wire Layout for IGBT Modules Considering Multicellular Electro-Thermal Effect," *IEEE Trans. Power Electron.*, vol. 37, no. 6, pp. 7299–7314, 2022.

[19] B. Czerny, I. Paul, G. Khatibi, and M. Thoben, "Experimental and analytical study of geometry effects on the fatigue life of Al bond wire interconnects," *Microelectron. Reliab.*, vol. 53, no. 9, pp. 1558–1562, Sep. 2013.

[20] P. Sun, C. Gong, X. Du, Y. Peng, B. Wang, and L. Zhou, "Condition Monitoring IGBT Module Bond Wires Fatigue Using Short-Circuit

Current Identification," *IEEE Trans. Power Electron.*, vol. 32, no. 5, pp. 3777–3786, 2017.

[21] Y. Huang, Y. Jia, Y. Luo, F. Xiao, and B. Liu, "Lifting-Off of Al Bonding Wires in IGBT Modules Under Power Cycling: Failure Mechanism and Lifetime Model," *IEEE Journal of Emerging and Selected Topics in Power Electronics*, vol. 8, no. 3, pp. 3162–3173, Jun. 2020.

[22] H. Meng, Y. Wang, X. Zheng, J. Chen, Y. Wu, A. Li, and Y. Huang, "Study of IGBTs Reliability Under Coupled Electrical-Thermal Environment," *IEEE Journal of Emerging and Selected Topics in Power Electronics*, vol. 9, no. 4, pp. 4260–4268, Apr. 2021.

[23] Q. Huang, C. Peng, S. F. M. Ellen, W. Zhu, and L. Wang, "A Finite Element Analysis on the Reliability of Heavy Bonding Wire for High-Power IGBT Module," *IEEE Trans. Compon. Packag. Manuf. Technol.*, vol. 11, no. 2, pp. 212–221, Oct. 2021.

[24] X. Dai, X. Yang, X. Wu, C. Tu, and G. Liu, "Analytical modeling of thermo-mechanical stress for bond wire of IGBT module," *Microelectron. Reliab.*, vol. 127, p. 114401, Dec. 2021.

[25] R. G. Budynas and J. K. Nisbett, *Shigley's Mechanical Engineering Design*. McGraw-Hill New York, 2011, vol. 9.

[26] L. Yang, P. A. Agyakwa, and C. M. Johnson, "Physics-of-Failure Lifetime Prediction Models for Wire Bond Interconnects in Power Electronic Modules," *IEEE Trans. Device Mater. Reliab.*, vol. 13, no. 1, pp. 9–17, Dec. 2013.

[27] J. Ye, X. Yang, X. Dai, X. Wu, K. Heng, and G. Liu, "A time-efficient strain-based lifetime prediction method for bond wires using vibration fatigue tests and finite element modeling," *IEEE Journal of Emerging and Selected Topics in Power Electronics*, vol. 12, no. 1, pp. 1011–1019, Nov. 2024.

[28] N. Dornic, Z. Khatir, S. H. Tran, A. Ibrahim, R. Lallemand, J. P. Ousten, J. Ewanchuk, and S. V. Mollov, "Stress-Based Model for Lifetime Estimation of Bond Wire Contacts Using Power Cycling Tests and Finite-Element Modeling," *IEEE Journal of Emerging and Selected Topics in Power Electronics*, vol. 7, no. 3, pp. 1659–1667, May 2019.

[29] M. Ouhab, N. Degrenne, and Y. Ito, "Creep Effect on the Crack Growth Rate of Wire Bonds in IGBT Power Modules," *IEEE Trans. Power Electron.*, vol. 39, no. 1, pp. 1482–1491, Jan. 2024.

[30] K. C. Nwanoro, H. Lu, C. Yin, and C. Bailey, "Advantages of the extended finite element method for the analysis of crack propagation in power modules," *Power Electronic Devices and Components*, vol. 4, p. 100027, Mar. 2023.

[31] J. Zhao, T. An, C. Fang, X. Bie, F. Qin, P. Chen, and Y. Dai, "A Study on the Effect of Microstructure Evolution of the Aluminum Metallization Layer on Its Electrical Performance During Power Cycling," *IEEE Trans. Power Electron.*, vol. 34, no. 11, pp. 11 036–11 045, 2019.

[32] P. Y. Pichon, J. Brandelero, J. L. Leslé, M. Ouhab, and V. Quemener, "Increasing the reliability of aluminum wirebonds by thermal treatments: Analysis and implementation," *IEEE Journal of Emerging and Selected Topics in Power Electronics*, vol. 11, no. 3, pp. 3502–3513, Jan. 2023.

[33] T. Yamaguchi, Y. Suto, N. Araki, M. Eto, F. Fischer, and A. Groth, "Investigation of failure mechanism of aluminum-scandium wire bond contact under active power cycle test," *Microelectron. Reliab.*, vol. 144, p. 114956, May 2023.

[34] M. Shqair, Z. Khatir, A. Ibrahim, M. Berkani, A. Halouani, and T. Hamieh, "A combined physicochemical-microstructural approach to predict the crack path at the topside interconnections in IGBT power devices," *Microelectron. Reliab.*, vol. 132, p. 114516, May 2022.

[35] J. Luo, S. Guan, B. Wan, M. Jiang, and G. Fu, "Research on IGBT bonding wires crack propagation at the macro and micro scales," *IEEE Access*, vol. 9, pp. 106 270–106 282, Jul. 2021.

[36] K. Yang, L. Zhou, F. Wu, G. Yang, L. Ding, K. Li, and X. Li, "Simulation of crack propagation in solder layer of IGBT device under temperature shock by viscoplastic phase field method," *Eng. Fract. Mech.*, vol. 284, p. 109260, May 2023.

[37] N. Moelans, B. Blanpain, and P. Wollants, "An introduction to phase-field modeling of microstructure evolution," *Calphad*, vol. 32, no. 2, pp. 268–294, Jun. 2008.

[38] A. Sadeghirad, K. Momeni, Y. Ji, X. Ren, L.-Q. Chen, and J. Lua, "Multiscale crystal-plasticity phase field and extended finite element methods for fatigue crack initiation and propagation modeling," *Int. J. Fract.*, vol. 216, no. 1, pp. 41–57, Feb. 2019.

[39] Y. Su, G. Fu, C. Liu, K. Zhang, L. Zhao, C. Liu, A. Liu, and J. Song, "Thermo-elasto-plastic phase-field modelling of mechanical behaviours of sintered nano-silver with randomly distributed micro-pores," *Comput. Methods Appl. Mech. Eng.*, vol. 378, p. 113729, May 2021.

[40] N. Dornic, A. Ibrahim, Z. Khatir, N. Degrenne, S. Mollov, and D. Ingrosso, "Analysis of the aging mechanism occurring at the bond-wire contact of IGBT power devices during power cycling," *Microelectron. Reliab.*, vol. 114, p. 113873, Nov. 2020.

[41] A. Laor, P. J. Herrell, and M. Mayer, "A Study on Measuring Contact Resistance of Ball Bonds on Thin Metallization," *IEEE Trans. Compon. Packag. Manuf. Technol.*, vol. 5, no. 5, pp. 704–708, 2015.

[42] F. Forndran, J. Heilmann, M. Metzler, M. Leicht, and B. Wunderle, "A Parametric Simulative Study for Lifetime Prediction of Sintered Silver Die Attach Under Different Accelerated Testing Conditions," in *2021 22nd International Conference on Thermal, Mechanical and Multi-Physics Simulation and Experiments in Microelectronics and Microsystems (EuroSimE)*, 2021, pp. 1–10.

[43] C. Miehe, F. Welschinger, and M. Hofacker, "Thermodynamically consistent phase-field models of fracture: Variational principles and multi-field FE implementations," *Int. J. Numer. Meth. Engng.*, vol. 83, no. 10, pp. 1273–1311, Aug. 2010.

[44] P. K. Kristensen, C. F. Niordson, and E. Martínez-Pañeda, "An assessment of phase field fracture: crack initiation and growth," *Philos. Trans. Royal Soc. A*, vol. 379, no. 2203, p. 20210021, Jun. 2021.

[45] M. Ambati, T. Gerasimov, and L. De Lorenzis, "A review on phase-field models of brittle fracture and a new fast hybrid formulation," *Comput. Mech.*, vol. 55, no. 2, pp. 383–405, Dec. 2015.

[46] M. Seiler, S. Keller, N. Kashaev, B. Klusemann, and M. Kästner, "Phase-field modelling for fatigue crack growth under laser shock peening-induced residual stresses," *Arch. Appl. Mech.*, vol. 91, no. 8, pp. 3709–3723, Mar. 2021.

[47] P. Carrara, M. Ambati, R. Alessi, and L. De Lorenzis, "A framework to model the fatigue behavior of brittle materials based on a variational phase-field approach," *Comput. Methods Appl. Mech. Eng.*, vol. 361, p. 112731, Apr. 2020.

[48] H. Bang, S.-k. Lee, C. Cho, and J. U. Cho, "Study on crack propagation of adhesively bonded DCB for aluminum foam using energy release rate," *J. Mech. Sci. Technol.*, vol. 29, no. 1, pp. 45–50, Jan. 2015.

[49] M. Kalina, V. Schöne, B. Spak, F. Paysan, E. Breitbarth, and M. Kästner, "Fatigue crack growth in anisotropic aluminium sheets – phase-field modelling and experimental validation," *Int. J. Fatigue*, vol. 176, p. 107874, Nov. 2023.

[50] A. Grams, J. Jaeschke, O. Wittler, B. Fabian, S. Thomas, and M. Schneider-Ramelow, "FEM-based combined degradation model of wire bond and die-attach for lifetime estimation of power electronics," *Microelectron. Reliab.*, vol. 111, p. 113683, Aug. 2020.

[51] H. Li, S. Chen, R. Yao, B. Zhou, W. Lai, J. Li, Z. Chen, and Y. Li, "Reliability Lifetime Prediction of SiC IGBT Devices with Different Packaging Approaches," in *The Proceedings of the 17th Annual Conference of China Electrotechnical Society*, K. Xie, J. Hu, Q. Yang, and J. Li, Eds. Singapore: Springer Nature Singapore, Mar. 2023. ISSN 978-981-99-0408-2 pp. 329–341.

[52] W. Velilla-Díaz, A. Pacheco-Sanjuan, and H. R. Zambrano, "The role of the grain boundary in the fracture toughness of aluminum bicrystal," *Comput. Mater. Sci.*, vol. 167, pp. 34–41, Sep. 2019.

[53] X. Tu, A. Ray, and S. Ghosh, "A coupled crystal plasticity FEM and phase-field model for crack evolution in microstructures of 7000 series aluminum alloys," *Eng. Fract. Mech.*, vol. 230, p. 106970, May 2020.

[54] M. J. Borden, C. V. Verhoosel, M. A. Scott, T. J. R. Hughes, and C. M. Landis, "A phase-field description of dynamic brittle fracture," *Comput. Methods Appl. Mech. Eng.*, vol. 217-220, pp. 77–95, Apr. 2012.

[55] H. Lu, C. Bailey, and C. Yin, "Design for reliability of power electronics modules," *Microelectron. Reliab.*, vol. 49, no. 9, pp. 1250–1255, Sep. 2009.

[56] P. A. Agyakwa, L. Yang, E. Arjmand, P. Evans, M. R. Corfield, and C. M. Johnson, "Damage Evolution in Al Wire Bonds Subjected to a Junction Temperature Fluctuation of 30 K," *J. Electron. Mater.*, vol. 45, no. 7, pp. 3659–3672, Apr. 2016.

[57] X. Cao, G. Q. Lu, and K. D. T. Ngo, "Planar Power Module With Low Thermal Impedance and Low Thermomechanical Stress," *IEEE Trans. Compon. Packag. Manuf. Technol.*, vol. 2, no. 8, pp. 1247–1259, 2012.

[58] B. Czerny and G. Khatibi, "Interface reliability and lifetime prediction of heavy aluminum wire bonds," *Microelectron. Reliab.*, vol. 58, pp. 65–72, Mar. 2016.

[59] J. H. Zhao, P. Su, M. Ding, S. Chopin, and P. S. Ho, "Microstructure-Based Stress Modeling of Tin Whisker Growth," *IEEE Trans. Electron. Packag. Manuf.*, vol. 29, no. 4, pp. 265–273, 2006.

[60] S. B. Liang, C. B. Ke, C. Wei, M. B. Zhou, and X. P. Zhang, "Study of the Influence of Elastic Anisotropy of Cu on Thermo-Mechanical Behavior and Cu Protrusion of Through Silicon Vias Using Combined Phase Field and Finite Element Methods," *IEEE Trans. Device Mater. Reliab.*, vol. 19, no. 2, pp. 322–332, Apr. 2019.

[61] L. Karanja, P. Pichon, J. Brandelero, and M. Legros, "Effect of post bonding annealing on the reliability of Al based wire bondings in IGBTs," *Microelectron. Reliab.*, vol. 138, p. 114647, 2022.

[62] E. Arjmand, P. A. Agyakwa, and C. M. Johnson, "Reliability of thick Al wire: A study of the effects of wire bonding parameters on thermal cycling degradation rate using non-destructive methods," *Microelectron. Reliab.*, vol. 54, no. 9, pp. 2006–2012, 2014.

[63] J. Onuki, M. Koizumi, and M. Suwa, "Reliability of thick Al wire bonds in IGBT modules for traction motor drives," *IEEE Trans. Adv. Packag.*, vol. 23, no. 1, pp. 108–112, Feb. 2000.

[64] A. Halouani, Z. Khatir, M. Shqair, A. Ibrahim, and P.-Y. Pichon, "An EBSD Study of Fatigue Crack Propagation in Bonded Aluminum Wires Cycled from 55°C to 85°C," *J. Electron. Mater.*, vol. 51, no. 12, pp. 7353–7365, 2022.

[65] Y. Yamada, Y. Takaku, Y. Yagi, I. Nakagawa, T. Atsumi, M. Shirai, I. Ohnuma, and K. Ishida, "Reliability of wire-bonding and solder joint for high temperature operation of power semiconductor device," *Microelectron. Reliab.*, vol. 47, no. 12, pp. 2147–2151, Dec. 2007.